⌘ *Author's Choice*

THE JOURNAL OF BIOLOGICAL CHEMISTRY VOL. 285, NO. 30, pp. 23265–23275, July 23, 2010

Membrane Trafficking of Large Conductance Calcium-activated Potassium Channels Is Regulated by Alternative Splicing of a Transplantable, Acidic Trafficking Motif in the RCK1-RCK2 Linker*

Received for publication, May 1, 2010 Published, JBC Papers in Press, May 17, 2010, DOI 10.1074/jbc.M110.139758

Lie Chen[‡], Owen Jeffries[‡], Iain C. M. Rowe[‡], Zhi Liang[‡], Hans-Guenther Knaus[§], Peter Ruth[¶], and Michael J. Shipston[‡1]

From the [‡]Centre for Integrative Physiology, College of Medicine & Veterinary Medicine, University of Edinburgh, Edinburgh EH8 9XD, Scotland, United Kingdom, the [§]Division for Molecular and Cellular Pharmacology, Department of Medical Genetics, Molecular and Clinical Pharmacology, Medical University Innsbruck, Peter-Mayr Strasse 1, 6020 Innsbruck, Austria, and [¶]Pharmacology and Toxicology, Institute of Pharmacy, University Tuebingen, 72076 Tuebingen, Germany

Trafficking of the pore-forming α-subunits of large conductance calcium- and voltage-activated potassium (BK) channels to the cell surface represents an important regulatory step in controlling BK channel function. Here, we identify multiple trafficking signals within the intracellular RCK1-RCK2 linker of the cytosolic C terminus of the channel that are required for efficient cell surface expression of the channel. In particular, an acidic cluster-like motif was essential for channel exit from the endoplasmic reticulum and subsequent cell surface expression. This motif could be transplanted onto a heterologous nonchannel protein to enhance cell surface expression by accelerating endoplasmic reticulum export. Importantly, we identified a human alternatively spliced BK channel variant, $hSlo\Delta_{579-664}$, in which these trafficking signals are excluded because of in-frame exon skipping. The $hSlo\Delta_{579-664}$ variant is expressed in multiple human tissues and cannot form functional channels at the cell surface even though it retains the putative RCK domains and downstream trafficking signals. Functionally, the $hSlo\Delta_{579-664}$ variant acts as a dominant negative subunit to suppress cell surface expression of BK channels. Thus alternative splicing of the intracellular RCK1-RCK2 linker plays a critical role in determining cell surface expression of BK channels by controlling the inclusion/exclusion of multiple trafficking motifs.

Large conductance calcium- and voltage-activated potassium (BK)[2] channels are widely expressed in mammalian cells where they play an important role in a diverse range of physiological processes ranging from the control of blood flow (1, 2) to the control of neuronal excitability and neurotransmitter release (3, 4). Indeed, a number of disorders, including hypertension (1, 2), epilepsy (5), incontinence (6), and sexual dysfunction (7) may result from perturbations of BK channel function. Correct cellular targeting of BK channels is an important regulatory mechanism, and changes in cell surface expression of these channels have been associated with different physiological demands, for example during pregnancy (8), with aging in coronary arteries (9), and with aldosterone-induced potassium secretion from the gut (10).

BK channels assemble as tetramers of pore-forming α-subunits, encoded by a single gene that undergoes extensive pre-mRNA splicing and can form complexes with a family of regulatory β-subunits (11). Increasing evidence suggests that alternative splicing at the N or C termini of BK channel α-subunits is a major determinant of BK channel cell surface expression. For example, inclusion of the alternatively spliced SV1 insert at the intracellular N terminus results in expression of an endoplasmic reticulum (ER) retention motif, CVLF, that prevents efficient export of the channel from the ER (12). In addition, the N-terminal mk44 variant (13) is endoproteolytically cleaved, resulting in plasma membrane localization of the N terminus of the mk44 variant and intracellular retention of the remaining cleaved pore-forming C terminus. Alternative splicing of the very C terminus of α-subunits is also a major determinant of cell surface expression, although the regulatory mechanisms are poorly understood (14). Alternative splicing that results in premature truncation of the BK channel α-subunit C terminus also results in intracellular retention of the channel as exemplified by the murine Δe23 (15) and rabbit rbSlo2 (16) as a result of a loss of putative C-terminal ER export signals as well as the RCK2 domain (15, 16).

Recent data also suggest that the intracellular C-terminal linker between the two predicted regulator of potassium conductance domains (see Fig. 1*a*, RCK1 and RCK2) is also an important determinant of BK channel surface expression. First, a rat splice variant SVcyt that has an ~80-amino acid in-frame deletion of the linker region is poorly expressed at the cell surface (17). Second, deletion of >30 amino acids in the linker regions produces nonfunctional channels that lack significant cell surface expression (18). However, the mechanism(s) re-

* This work was supported by the Wellcome Trust.
⌘ *Author's Choice*—Final version full access.
[1] To whom correspondence should be addressed: Centre for Integrative Physiology, Hugh Robson Bldg., University of Edinburgh, Edinburgh EH8 9XD, UK. Tel.: 44-131-6503253; Fax: 44-131-6506521; E-mail: mike.shipston@ed.ac.uk.
[2] The abbreviations used are: BK channel, large conductance calcium- and voltage-activated potassium channel; ER, endoplasmic reticulum; HEK, human embryonic kidney; IP, immunoprecipitation; NORS, no regular secondary structure; RCK, regulator of potassium conductance; HA, hemagglutinin; eYFP, enhanced yellow fluorescent protein; ANOVA, analysis of variance.

sponsible for the trafficking defect in these linker deletion mutants are not known.

In this report, we identify multiple trafficking motifs within the intracellular RCK1-RCK2 linker that control cell surface expression of BK channel α-subunits expressed in mammalian cells. Importantly, we reveal an acidic cluster-like motif (DD*XX*D*XXX*I) that is critical for cell surface expression of the channel that can be transplanted to a heterologous nonchannel protein to enhance membrane expression. Furthermore, we have isolated a widely expressed human BK channel splice variant (hSloΔ$_{579-664}$), in which the exons encoding these trafficking motifs are excluded. Exclusion of these exons results in an in-frame 86-amino acid deletion that encodes a channel that is a dominant negative of cell surface expression. Taken together, our data reveal that alternative splicing of the RCK1-RCK2 linker region, resulting in inclusion/exclusion of multiple trafficking motifs, is an important determinant of BK channel cell surface expression.

EXPERIMENTAL PROCEDURES

Cloning of the hSloΔ$_{579-664}$ Variant, Channel Mutagenesis, and GABA$_B$R1a Constructs—A human tissue rapid scan cDNA pool (Origene) was screened for splice variants by PCR-amplifying a region between exons 15 and 25 (see Fig. 1*a*) of the human BK channel α-subunit with the forward and reverse primer pairs: 5′-TTgCCAACCTCTTCTCC-3′ and 5′-gTgCTTgAgCTCATGggTAAT-3′, respectively. PCR amplicons were cloned into the pCR®II-TOPO vector (Invitrogen). To generate full-length BK channel α-subunit cDNAs, the novel variant *hSloΔ$_{579-664}$* amplicon from pCR®II-TOPO was subcloned into the murine BK channel α-subunit with an N-terminal FLAG tag and/or a C-terminal HA or eYFP tag described previously (15, 19–21). Site-directed mutations were generated using the QuikChange® site-directed mutagenesis kit (Stratagene) using standard procedures. All of the amino acid numbering is based on the human BK channel α-subunit (*hSlo*) with start methionine at MDALI (accession number AAD31173).

GABA$_B$R1a receptor plasmids with N-terminal extracellular HA-GABA$_B$R1a and HA-GABA$_B$R1a-ASRR plasmids were kind gifts from Prof. Lily Jan (University of California at San Francisco) (22). To engineer the DD*XX*D*XXX*I sequence at the C terminus of both constructs, we PCR-amplified the C terminus with forward (5′-TTTgCCAAggAggAACCAAAg-3′) and reverse (5′-CTCTAgATCAAATTCTTTTgggATCTgTgACgTCATCCTTgTAAAgCA-3′) primers. The reverse primer encodes a DD*XX*D*XXX*I sequence, and the resultant PCR amplicons were ligated into the GABA$_B$R1a plasmids using ClaI and XbaI restriction sites. All of the sequences were confirmed by automated sequencing on both strands (MWG-Biotech).

Quantitative Real Time-PCR TaqMan™ Assay—Quantitative analysis of the human BK channel variant transcripts was performed using a TaqMan™ assay (15). The probes and primer sets of total *hSlo* and *hSloΔ$_{579-664}$* were designed with Primer Express v1.2. TaqMan™ probes, labeled at the 5′ end with 6-carboxyfluorescein and at the 3′ end with 6-carboxytetramethylrhodamine were synthesized by ABI (Applied Biosystems). The following TaqMan™ assays were used to screen cDNAs from human tissues: for total *hSlo*: forward, 5′-gTCTCAAATgAAATgTACACAgAATATCTCT-3′; reverse, 5′-gCAgACTTgTACTCAATggCTATCA-3′; and probe, 5′-CCTTCgTgggTCTgTCCTTCCCTACTgTT-3′; and for hSloΔ$_{579-664}$: forward, 5′-gCTCCTAATgATAgCCATTgAgTACA-3′; reverse, 5′-TgATCATTgCCAggAATTAACAAg-3′; and probe, 5′-CCAACCgAgAgAgCCggCATgA-3′. The efficiency, correlation coefficient (R^2), and limit of detection for each TaqMan™ assay were: for total *hSlo*: 2.03, 0.97, and <0.3 fg of cDNA; and for *hSloΔ$_{579-664}$*: 2.02, 0.99, and <0.3 fg of cDNA. All of the data were analyzed using ABI Prism 7000 SDS software version 1.0 (Applied Biosystems). Transcript expression was determined from standard curves generated using dilutions of the respective splice variant plasmid DNA, and variant expression is given as a percentage of total BK channel transcripts in each tissue.

HEK293 Cell Culture and Immunofluorescence—HEK293 cells were maintained and transfected as described (15, 21). Cell surface labeling of the N-terminal FLAG epitope of BK channels in nonpermeabilized HEK293 cells was performed (15) using mouse monoclonal anti-FLAG M2 antibody (50 μg/ml Sigma) and Alexa-594-conjugated anti-mouse rabbit IgG (Molecular Probes). The cells were subsequently fixed in 4% paraformaldehyde for 30 min, permeabilized with 0.3% Triton X-100 for 10 min, and blocked with phosphate-buffered saline containing 3% bovine serum albumin plus 0.05% Triton X-100 for 30 min. The intracellular C-terminal HA epitope tag was detected using 0.5 μg/ml anti-HA polyclonal rabbit antibody (Zymed Laboratories Inc.) and Alexa-488-conjugated anti-rabbit chicken IgG (Molecular Probes), and the cells were mounted using Mowiol.

Confocal images were acquired on a Zeiss LSM510 laser scanning microscope using a 63× oil Plan Apochromat (NA = 1.4) objective lens in multi-tracking mode to minimize channel cross-talk and analyzed as described (19). FLAG surface expression was quantified in two ways: (i) using a threshold method to detect the total number of all transfected cells that displayed FLAG surface expression in each group and (ii) using absolute measures based on ratios of surface FLAG (extracellular) fluorescence to intracellular signal (eYFP or HA as appropriate) in a random subset of all cells analyzed using Image J. The data were then normalized to the corresponding control group (100%) as indicated in the respective figure legend. In these experimental paradigms the data obtained for relative surface expression using the threshold method were quantitatively the same as using the absolute ratio measure, therefore these data were pooled. In Fig. 2*b* >90% of all of the transfected cells display surface expression of the respective e22 and zero variants; however, we could not detect surface expression of the hSloΔ$_{579-664}$ variant in any cell examined. The same approach was used for the HA-tagged GABA$_B$R1a receptor constructs except that distinct fluorescent second antibodies directed against the N-terminal HA tag were used in nonpermeabilized and permeabilized conditions.

To assay co-localization of the channels with the ER, HEK293 cells were co-transfected with the HA-tagged channels and the pdsRed-ER (Clontech) vector. The HA tag was detected as above, and confocal images taken at Nyquist sampling rates were collected and analyzed as described previously (23). The

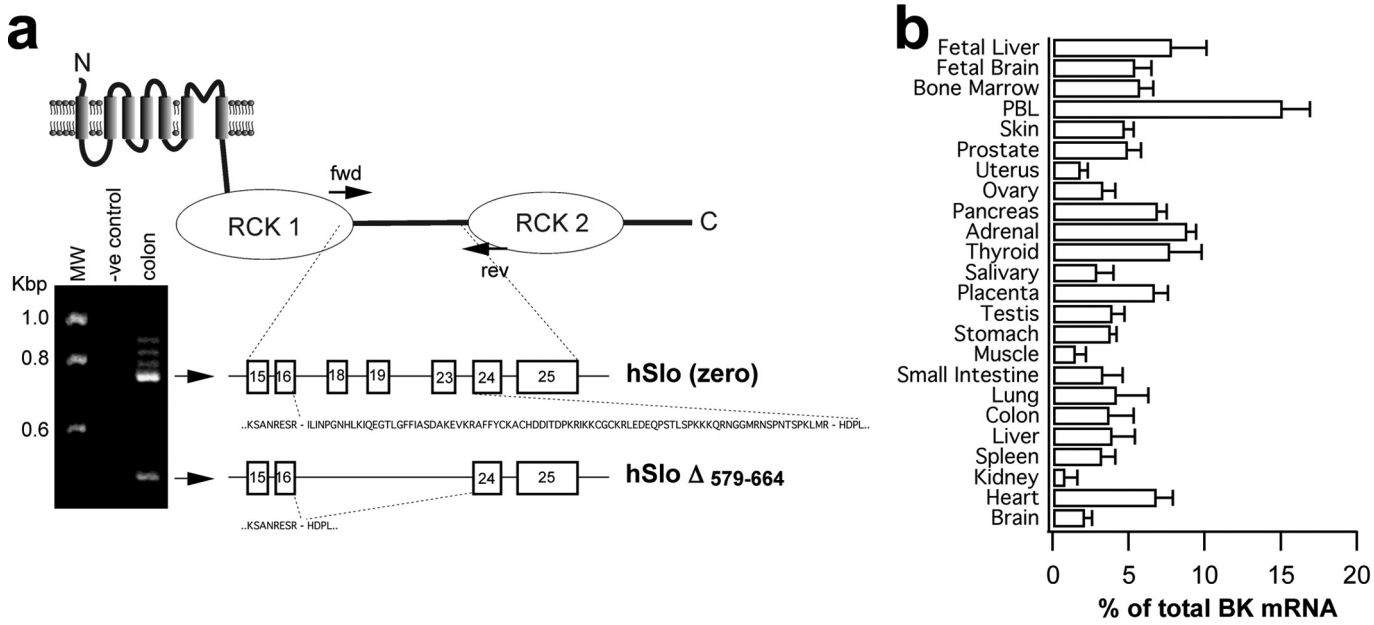

FIGURE 1. **Cloning and tissue mRNA expression of a human BK channel splice variant, hSlo$\Delta_{579-664}$, with an in-frame 86-amino acid deletion in the RCK1-RCK2 linker region.** *a*, schematic illustrating the topology of a BK channel α-subunit with an extracellular N terminus and a large intracellular C terminus. Exon (*numbered open boxes*) structure for the hSlo zero variant (with no alternatively spliced inserts in this region) and the hSlo$\Delta_{579-664}$ variant are shown. The representative agarose gel illustrates multiple amplicons generated by the forward (*fwd*) and reverse (*rev*) primers in human colon cDNA. The *upper* and *lower arrows* indicate the human hSlo zero and hSlo$\Delta_{579-664}$ variants, respectively, with the corresponding amino acid sequence. hSlo$\Delta_{579-664}$ results from an 86-amino acid in-frame deletion; thus the rest of the intracellular C terminus including RCK2, the calcium bowl, and other essential trafficking motifs for cell surface expression are retained. *b*, hSlo$\Delta_{579-664}$ variant mRNA levels expressed as percentages of total BK channel mRNA transcripts in selected human tissues determined using TaqMan™ analysis. All of the data are the means ± S.E., $n = 3$/tissue region. *MW*, molecular mass.

images were deconvolved using Huygens software (Scientific Volume Imaging) and analyzed using ImageJ (National Institutes of Health) to obtain the Pearson's correlation coefficient. Coefficients range from 1 to −1. A value of 1 indicates a complete positive correlation between the two channels, whereas −1 stands for a negative correlation.

Immunoprecipitation and Western Blotting—Immunoprecipitation (IP) and Western blotting were performed as previously described (15). HEK293 cells were solubilized at 4 °C in lysis buffer (NLB) containing 150 mM NaCl, 50 mM HEPES, pH 7.5, 1.5 mM $MgCl_2$, 10 mM sodium pyrophosphate, 20 mM NaF, 1 mM EDTA, 5 mM EGTA, 10% (v/v) glycerol, 1% Triton X-100, and complete protease inhibitor mixture (Roche Applied Science). After preclearing, the channels were immunoprecipitated with anti-HA (rabbit polyclonal; Zymed Laboratories Inc.) or anti-FLAG M2 monoclonal mouse antibody (Sigma). Negative control IPs included: (i) IP of mock transfected cells; (ii) IP from cells transfected with channels without the cognate epitope tag; (iii) beads alone; or (iv) irrelevant IP antibody. Bound complexes were separated through a 10% SDS-PAGE gel and electroblotted to polyvinylidene difluoride membrane and probed for the HA or FLAG tag using rabbit polyclonal anti-HA (Zymed Laboratories Inc.), 0.5 μg/ml, or mouse monoclonal anti-FLAG M2 (Sigma), 20 μg/ml. The blots were incubated with horseradish peroxidase-conjugated anti-rabbit IgG/or anti-mouse IgG secondary antibody (1/5000 dilution; Sigma) for 1 h at room temperature. The signals were detected using ECL.

Cell Surface Biotinylation Assay—Plasmids expressing HA- or eYFP-tagged BK channels were transiently transfected into HEK293 cells with Exgen 500 (Fermentas). 48 h post-transfection, the cells were washed three times with Hanks' buffered salt solution and then incubated on ice for 2 h in the presence of 5 μg/ml of Sulfo-NHS-LC-biotin (Pierce). After three washes in ice-cold 100 mM glycine in Hanks' buffered salt solution, the cells were lysed in NLB lysis buffer with protease inhibitor mixture (Roche Applied Science). Biotinylated cell lysates were incubated with streptavidin-immobilized beads (Pierce) overnight at 4 °C, washed three times with cold Hanks' buffered salt solution, and washed once with water. The biotinylated membrane BK channel proteins were removed from the beads by incubating at 45 °C for 15 min in 2× Laemmli protein sample buffer, separated by SDS-PAGE, and detected with anti-HA or green fluorescent protein antibody using Western blot. Parallel control biotinylation assays were conducted with: (i) mock transfected cells, (ii) cells immunoprecipitated with streptavidin beads in the absence of biotin incubation, and (iii) immunoprecipitation with an irrelevant antibody.

Fluorescent Membrane Potential Assay—The membrane potential assays were performed in transfected HEK293 cells using FLIPR® membrane potential blue dye (Molecular Devices, Sunnyvale, CA) essentially as described (24). Briefly, the cells were plated in black-walled, clear-bottomed 96-well plates and loaded with dye for 30 min at 37 °C. The assays were performed at 22 °C using a FlexStation® II system (Molecular Devices), and the channels were activated by applying 1 μM of the calcium ionophore, ionomycin, 16 s after the experiment began. The fluorescence changes were read at high sensitivity at 180 s at intervals of 1.52 s with excitation/emission wavelengths of 530/565 nm, respectively. A decrease in relative fluorescent units, with respect

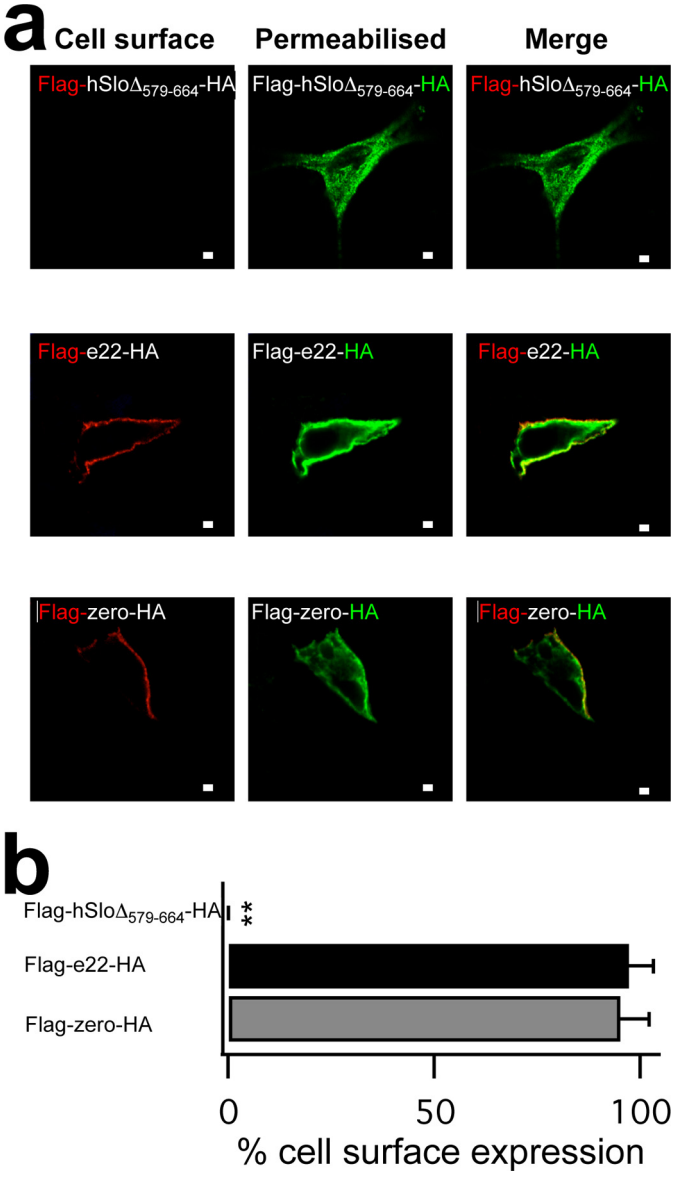

FIGURE 2. **Lack of cell surface expression of the hSloΔ$_{579-664}$ variant.** *a*, representative confocal images of HEK293 cells expressing FLAG-hSloΔ$_{579-664}$-HA (*top panels*), FLAG-e22-HA (*middle panels*), or FLAG-zero-HA (*bottom panels*). The extracellular FLAG epitope was labeled (*red*) under nonpermeabilized conditions (cell surface) with the C-terminal HA epitope tag (*green*) labeled following cell permeabilization. FLAG and HA labeling from the same cell are then overlaid (*Merge*). The FLAG-e22-HA construct is a splice variant with an alternatively spliced exon (exon 22) included between exons 19 and 23. The *scale bars* are 2 μm. *b*, quantification of surface expression expressed as a percentage of the total number of transfected cells with detectable cell surface (FLAG) expression for experiments as performed in *a*. The data are the means ± S.E. from a minimum of three independent experiments with >600 cells analyzed/group. **, $p < 0.01$, ANOVA with post hoc Dunnett's test compared with FLAG-zero-HA construct.

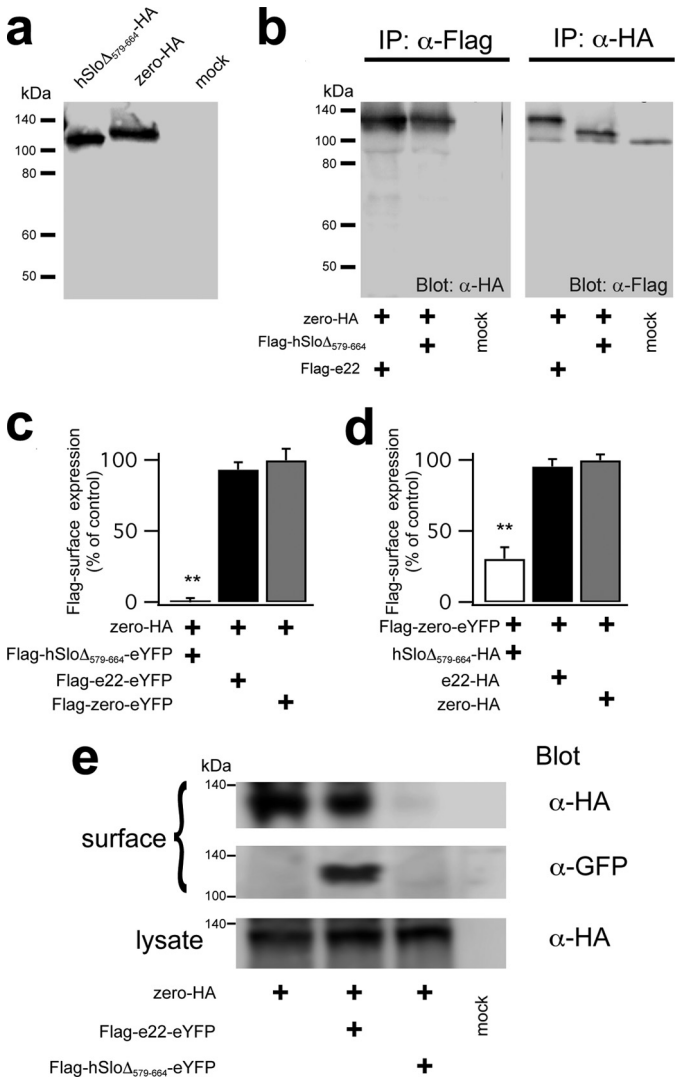

FIGURE 3. **The hSloΔ$_{579-664}$ variant is a dominant negative of cell surface expression.** *a*, Western blot of total cell lysates from the FLAG-hSloΔ$_{579-664}$-HA and FLAG-zero-HA variants expressed in HEK293 cells. *b*, representative blots from co-immunoprecipitation (*IP*) experiments from HEK293 cells co-expressing the zero-HA variant with either the FLAG-hSloΔ$_{579-664}$ or FLAG-e22 variants. *Left panel*, channels were immunoprecipitated with mouse anti-FLAG M2 antibody, and blots were probed with rabbit anti-HA antibody. *Right panel*, channels were immunoprecipitated with rabbit anti-HA antibody and probed with mouse anti-FLAG M2 antibody. *c*, zero-HA subunits were co-expressed with either FLAG-hSloΔ$_{579-664}$-eYFP, FLAG-e22-eYFP, or FLAG-zero-eYFP channels in HEK293 cells, and cell surface (FLAG) expression was quantified. *d*, FLAG-zero-eYFP subunits were co-expressed with either hSloΔ$_{579-664}$-HA, e22-HA or zero-HA channels in HEK293 cells. In *c* and *d*, the data are the cell surface FLAG staining values expressed as percentages of control (surface FLAG-zero-eYFP levels when co-expressed with the zero-HA construct) under nonpermeabilized conditions. *e*, representative Western blots of HA or green fluorescent protein immunoreactivity from cell surface biotinylation assays of HEK293 cells expressing the indicated constructs and corresponding whole cell lysates. All data are the means ± S.E. from a minimum of six independent experiments with >700 cells analyzed/group in *c* and *d* and three independent experiments in *a*, *b*, and *e*. **, $p < 0.01$, ANOVA with post hoc Dunnett's test compared with other groups.

to mock transfected HEK293 cells, reflects membrane hyperpolarization (BK channel activation).

BK channel activation was fully blocked by 1–10 μM paxilline (not shown; see Ref. 23). The data were analyzed with SoftMax Pro and exported to Igor Pro, Microsoft Excel, and/or Prism for further analysis. To compare between mutants, the relative fluorescent units were determined 70 s into the assay. The response of each channel mutant was then normalized to the hyperpolarization response of the zero channel (100%).

Statistics—Statistical analysis was performed using Igor Pro v6.0 using a one-way ANOVA with a Dunnett's post hoc test for significance between groups at $p < 0.05$.

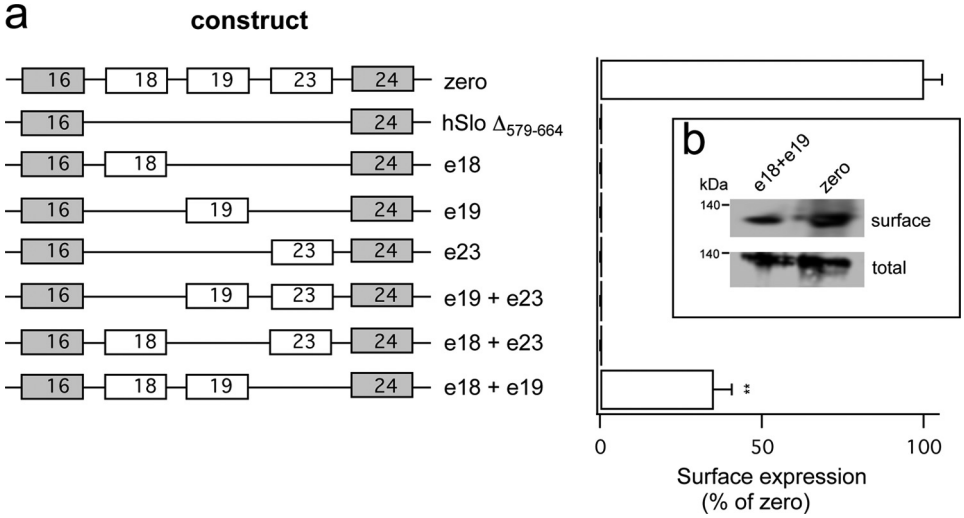

FIGURE 4. **Exon 18 and exon 19, but not exon 23, are essential for BK channel cell surface expression.** *a*, in-frame deletion mutants of exons 18, 19, and 23 that are excluded in the hSlo$\Delta_{579-664}$ trafficking-deficient variant were expressed in HEK293 cells. Constructs contained an N-terminal extracellular FLAG tag and a C-terminal HA tag. Cell surface expression was assayed in imaging experiments under nonpermeabilized conditions by probing for the FLAG tag as in Fig. 3. The data are expressed as percentages of control FLAG-zero-HA cell surface expression. *b*, *inset*, representative Western blots of HA immunoreactivity from cell surface biotinylation assays of HEK293 cells expressing the zero or e18 + e19 constructs and corresponding whole cell lysates. All of the data are the means ± S.E. from a minimum of three independent experiments with >650 cells analyzed/group. **, $p < 0.01$, ANOVA with post hoc Dunnett's test compared with all other groups.

RESULTS

Cloning of a Human BK Channel Splice Variant with an 86-Amino Acid Deletion in the RCK1-RCK2 Linker, hSlo$\Delta_{579-664}$—We isolated a human BK channel splice variant, hSlo$\Delta_{579-664}$, from human colon tissue cDNAs using reverse transcription-PCR primers to amplify the region spanning exons 15–25 (Fig. 1*a*) that encompasses the C-terminal region of the predicted RCK1 domain and the unstructured (NORS) RCK1-RCK2 linker (18). Using these primers, multiple sized amplicons were generated that encoded for previously identified splice variants at sites of splicing C1 and C2, including the human zero variant that lacks inserts at these sites (Fig. 1*a*). From the amplicons we identified a significantly smaller sized product than the insertless zero variant that results from skipping three exons, producing a deletion of 86 amino acids between isoleucine 579 and arginine 664. The exclusion of exons 18, 19, and 23 results in splicing from exons 16 to 24, leading to an in-frame deletion with the splice variant retaining the more C-terminal RCK2 domain (25), the "calcium bowl" required for calcium sensitivity of the channels, as well as C-terminal ER export signals (16). We have named this splice variant hSlo$\Delta_{579-664}$ (based on amino acid numbering system for hSlo variant starting at MDALI, accession number AAD31173). This variant represents the human ortholog of the previously described rat splice variant SVcyt (17). To quantify the expression of mRNAs encoding the hSlo$\Delta_{579-664}$ splice variant in different human tissues, we designed and carried out TaqMan™ real time quantitative PCR assays. Total BK channel transcripts (normalized to β-actin) were highest in prostate, brain, muscle, and uterus and lowest in heart, thyroid, plasma blood cell, and bone marrow (data not shown). In most tissues, the proportion of total BK transcripts that expressed the new variant, hSlo$\Delta_{579-664}$, was less than 10% (Fig. 1*b*). The proportional expression of the new variant hSlo$\Delta_{579-664}$, was highest in those tissues, such as heart, thyroid, plasma blood cell, and fetal liver, which express the lowest total BK channel transcript levels.

hSlo$\Delta_{579-664}$ Is a Dominant Negative of Cell Surface Expression—Fusion of green fluorescent protein to the C terminus of the rat SVcyt homolog resulted in trapping of the SVcyt variant into the cytoplasm of mammalian cells with no detectable current (17). In addition, recent data suggest that deletion of >30 amino acids in the RCK1-RCK2 linker results in nonfunctional channels (18). To address whether the hSlo$\Delta_{579-664}$ splice variant could be expressed at the cell surface and form functional channels, we took two approaches.

First, we asked whether single channel/macropatch BK currents were detectable in HEK293 cells expressing the hSlo$\Delta_{579-664}$ variant using both untagged constructs as well as channels with an N-terminal FLAG epitope and a C-terminal HA epitope. No identifiable BK channel currents were observed in either 39 cell attached patches or 29 excised inside out patches exposed over the potential range ±100 mV and with >100 μM free calcium. In contrast, using the zero variant under identical conditions, we observed multiple channels in >55% of patches in cell-attached or excised patch configurations (data not shown). A similar lack of functional expression was also observed in fluorescent membrane potential assays (*e.g.* see Fig. 8).

Second, to determine whether the hSlo$\Delta_{579-664}$ was expressed at the cell surface, we transfected the FLAG-hSlo$\Delta_{579-664}$-HA construct in HEK293 cells (Fig. 2). In nonpermeabilized cells, the extracellular N-terminal FLAG tag could not be detected in immunofluorescence assays in any cell ($n > 1500$ cells analyzed), suggesting that the channel could not insert into the plasma membrane (Fig. 2). In contrast, in the same experiments two distinct splice variants (FLAG-e22-HA and FLAG-zero-HA variants (15)) showed robust FLAG tag expression at the cell surface in >90% of nonpermeabilized, transfected cells (Fig. 2). To confirm that the lack of FLAG epitope detection with the FLAG-hSlo$\Delta_{579-664}$-HA variant was not due to a lack of protein expression, we analyzed expression of the HA epitope tag in the same cells under permeabilized conditions (Fig. 2*a*). The hSlo$\Delta_{579-664}$ variant displayed robust expression in both immunocytochemical (Fig. 2*a*) and Western blot (Fig. 3*a*) assays. Indeed, total cellular protein levels of the hSlo$\Delta_{579-664}$ construct were not significantly different from that observed with zero constructs, suggesting that the lack of cell surface expression does not result from decreased synthesis and/or increased degradation of the hSlo$\Delta_{579-664}$

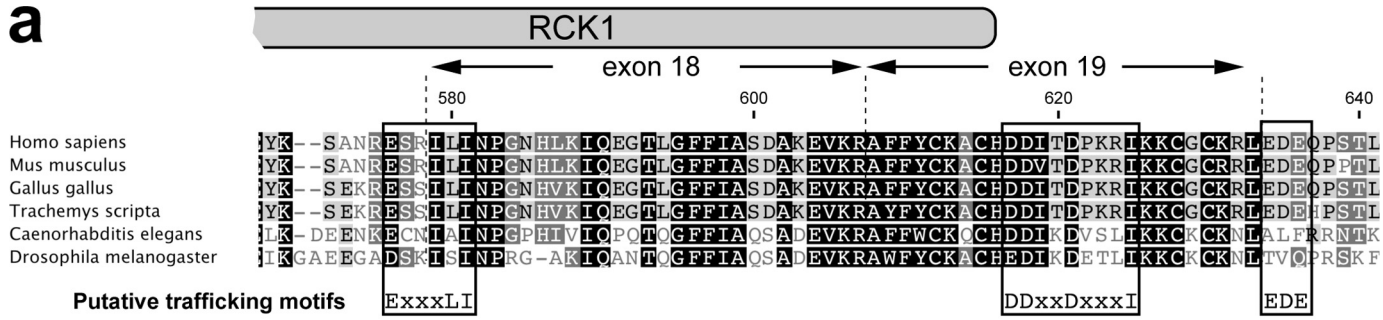
a
RCK1
exon 18
exon 19
580
600
620
640
Homo sapiens
Mus musculus
Gallus gallus
Trachemys scripta
Caenorhabditis elegans
Drosophila melanogaster
Putative trafficking motifs
ExxxLI
DDxxDxxxI
EDE

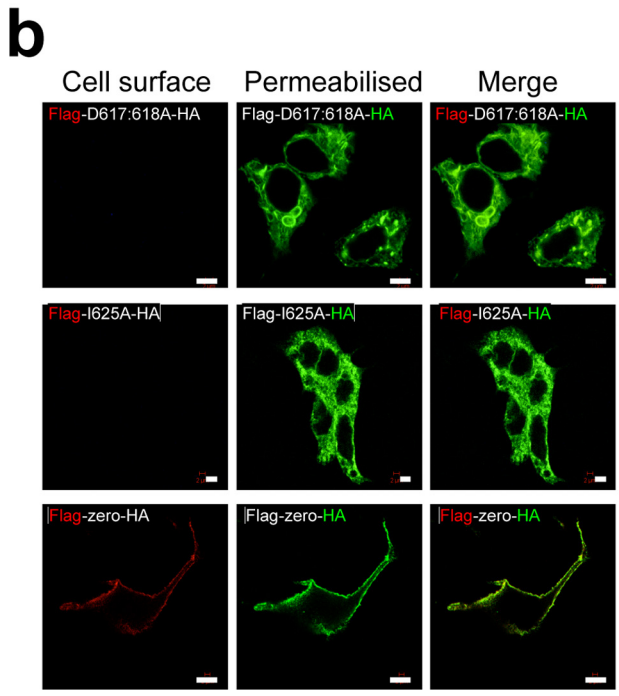
b
Cell surface
Permeabilised
Merge
Flag-D617:618A-HA
Flag-I625A-HA
Flag-zero-HA

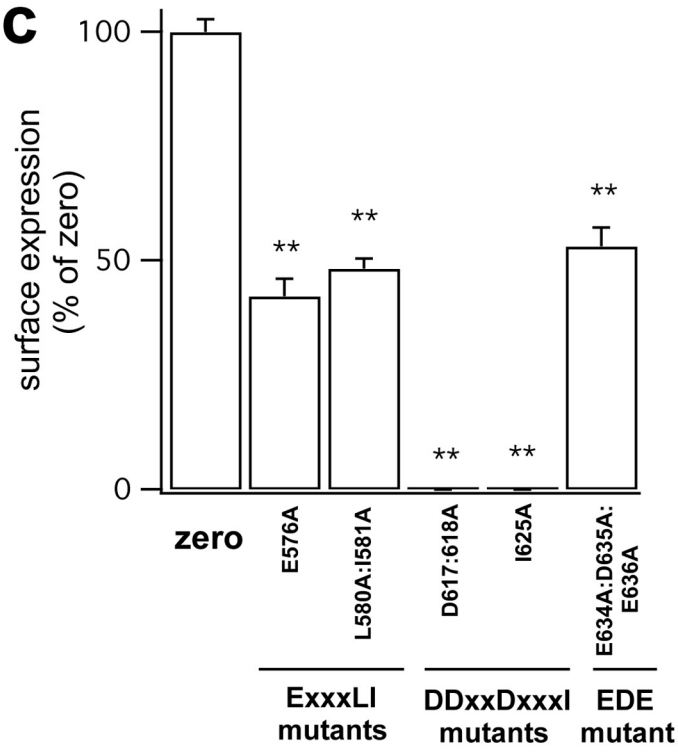
c
surface expression (% of zero)
100
50
0
**
zero
E576A
L580A:I581A
D617:618A
I625A
E634A:D635A: E636A
ExxxLI mutants
DDxxDxxxI mutants
EDE mutant

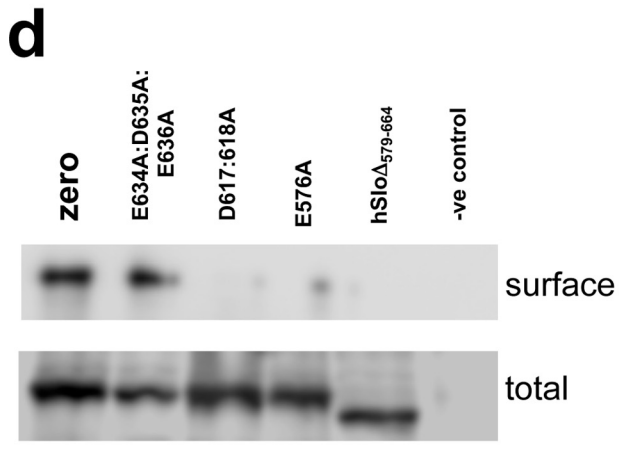
d
zero
E634A:D635A: E636A
D617:618A
E576A
hSloΔ579-664
-ve control
surface
total

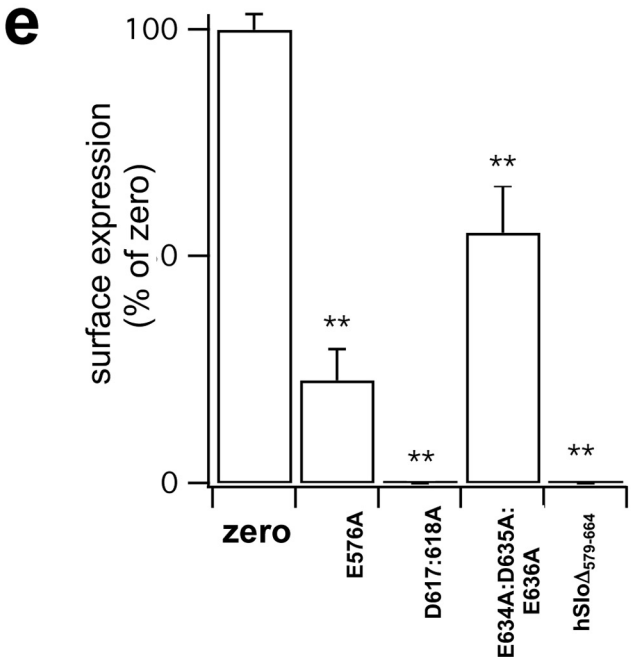
e
surface expression (% of zero)
100
0
**
zero
E576A
D617:618A
E634A:D635A: E636A
hSloΔ579-664

variant (Fig. 3*a*). As expected from the 86-amino acid deletion, the hSlo$\Delta_{579-664}$ variant was detectable as an ~110-kDa immunoreactive band in Western blots (Fig. 3*a*). Probing for the hSlo$\Delta_{579-664}$ variant in intact HEK293 cells revealed that the hSlo$\Delta_{579-664}$ variant was retained in intracellular structures within the cytoplasm. Although a functional role for intracellular BK channels has been reported, for example in mitochondria (26), the hSlo$\Delta_{579-664}$ variant did not co-localize with mitochondrial markers (data not shown) in HEK293 cells but was extensively trapped in the ER (Figs. 5 and 6). Taken together, these data suggest that a homomeric hSlo$\Delta_{579-664}$ variant is trafficking-deficient, is trapped intracellularly, and is thus unable to form functional channels at the plasma membrane.

Because BK channels exist as tetramers, the hSlo$\Delta_{579-664}$ variant may be able to assemble with other BK channel splice variant α-subunits. To test this idea, we first performed reciprocal co-immunoprecipitation assays by expressing a FLAG-tagged hSlo$\Delta_{579-664}$ variant with HA-tagged zero subunits (Fig. 3*b*). Co-expression of the FLAG-hSlo$\Delta_{579-664}$ variant with the zero-HA variant resulted in robust, reciprocal co-immunoprecipitation of both variants (Fig. 3*b*). Similar co-immunoprecipitation was observed using the e22 splice variant (Fig. 3*b*), which also shows robust cell surface expression (Fig. 2), or between hSlo$\Delta_{579-664}$-HA and FLAG-zero (not shown). Thus hSlo$\Delta_{579-664}$ can heteromultimerize with other BK channel α-subunits, suggesting that channel assembly *per se* is not compromised.

We next asked whether cell surface expression of the hSlo$\Delta_{579-664}$ variant may be rescued upon co-expression with cell surface trafficking competent α-subunits. We thus expressed a FLAG-hSlo$\Delta_{579-664}$-eYFP variant with the zero-HA construct to allow simultaneous monitoring of expression of both constructs in the same cell while assaying for the external FLAG epitope tag (Fig. 3*c*) in nonpermeabilized cell surface assays. However, no significant rescue of the hSlo$\Delta_{579-664}$ variant was observed. As controls, the co-expression of zero-HA had no effect on either FLAG-e22-eYFP or FLAG-zero-eYFP surface expression (Fig. 3*c*). This was confirmed in cell surface biotinylation assays (Fig. 3*e*).

Because other BK channel α-subunit splice variants may act as dominant negative regulators of cell surface expression (15, 27), we thus asked whether the hSlo$\Delta_{579-664}$ variant could control cell surface expression of other variants. Using a FLAG-tagged zero-eYFP construct (FLAG-zero-eYFP) co-expressed with the hSlo$\Delta_{579-664}$-HA, zero-HA, or e22-HA variants allowed us to assay cells in which both constructs were co-expressed while independently assaying for cell surface expression using the FLAG epitope. Co-expression of FLAG-zero-eYFP and hSlo$\Delta_{579-664}$-HA constructs resulted in a significant reduction (>60%) of cell surface expression of FLAG-zero-eYFP (Fig. 3*d*). The effect of hSlo$\Delta_{579-664}$-HA was not due to an overexpression artifact because co-expression of FLAG-zero-eYFP with e22-HA was without effect on FLAG-zero-eYFP surface expression.

Identical data were obtained in cells co-expressing FLAG-zero channels lacking the eYFP tag with hSlo$\Delta_{579-664}$-HA; surface FLAG expression in the presence of hSlo$\Delta_{579-664}$-HA was 37.6 ± 4.2% of FLAG-zero, whereas co-expression with e22-HA resulted in FLAG surface expression that was 95.0 ± 5.6% of FLAG-zero channels. The residual cell surface expression of FLAG-zero channels in these immunofluorescence assays when co-expressed with hSlo$\Delta_{579-664}$ most likely results from formation of homomultimers of FLAG-zero at the cell surface because in both imaging and cell surface biotinylation assays (Fig. 3*e*), we could not detect hSlo$\Delta_{579-664}$ at the cell surface. As hSlo$\Delta_{579-664}$ and zero channels express at similar levels in HEK293 cells (Fig. 3*a*); this may indicate that the efficiency of heteromultimerization is compromised when channel subunits incorporate the hSlo$\Delta_{579-664}$ variant.

The dominant negative effects of hSlo$\Delta_{579-664}$ data were recapitulated with biochemical assays of cell surface biotinylation (Fig. 3*e*). No significant surface expression could be detected of either zero-HA or FLAG-hSlo$\Delta_{579-664}$-eYFP in cells expressing both constructs supporting the dominant negative role of hSlo$\Delta_{579-664}$. In contrast, robust surface expression of both FLAG-e22-eYFP and zero-HA could be detected in cells co-expressing these constructs (Fig. 3*e*). These data suggest that the hSlo$\Delta_{579-664}$ variant acts as a dominant negative of cell surface expression.

Exons 18 and 19, but Not Exon 23, Are Essential for Cell Surface Expression—Because the hSlo$\Delta_{579-664}$ variant could heteromultimerize with other BK channel α-subunits and act as a dominant negative of cell surface expression, we hypothesized that the mechanism underlying the trafficking defect was not a result of incorrect channel assembly, because of the 86-amino acid deletion, but rather arose from the deletion of essential, discrete trafficking signals within the RCK-RCK2 linker upon exclusion of exons 18, 19, and 23 in the hSlo$\Delta_{579-664}$ variant.

As a first step to test this idea, we assayed the contribution of the individual exons 18, 19, and 23, which are excluded in the hSlo$\Delta_{579-664}$ variant, to cell surface expression by determining

FIGURE 5. **An acidic cluster-like motif in exon 19 is essential for cell surface expression.** *a*, ClustalW sequence alignment of exons 18 and exon 19 from human (*Homo sapiens*, accession number AAD31173), mouse (*Mus musculus*, accession number AAL69971), chicken (*Gallus gallus*, accession number NP_989555), turtle (*Trachemys scripta*, accession number AAC41281), worm (*Caenorhabditis elegans*, accession number NP_001024259), and fly (*Drosophila melanogaster*, accession number NP_524486). The exons form the extreme C terminus of the computationally predicted RCK1 domain and the start of the unstructured RCK1-RCK2 linker. Three putative trafficking/sorting motifs predicted in this region are shown with only the acidic DD*XXD**XXX*I motif fully conserved across phyla. Amino acid numbering is based on the amino acid sequence of the human sequence AAD31173 that starts with MDALI. *b*, representative confocal sections from HEK293 cells transfected with the DD*XXD**XXX*I mutants (D617A/D618A and I625A) and zero channels with the N-terminal epitope labeled under nonpermeabilized conditions and the intracellular C-terminal HA tag under permeabilized conditions. The *scale bars* are 2 μm. *c*, summary bar chart of cell surface FLAG expression of trafficking/sorting motif mutants in which amino acids within the proposed motifs are mutated to alanine. Cell surface expression is expressed as a percentage of the FLAG-zero-HA construct using FLAG surface expression in nonpermeabilized assays as in Fig. 2. *d*, representative Western blots of HA immunoreactivity from cell surface biotinylation assays of HEK293 cells expressing the corresponding constructs and whole cell lysates. *e*, summary bar chart of cell surface biotinylation data as in *d*. All of the data are the means ± S.E. from a minimum of three independent experiments with >720 cells analyzed/group in *c*. **, $p < 0.01$, ANOVA with post hoc Dunnett's test compared with the zero channel.

whether cell surface expression of the hSlo$\Delta_{579-664}$ variant could be rescued by the reinsertion of single or double exons in combination (Fig. 4). We thus generated a number of chimaeras in which one or two exons were ligated in-frame between exons 16 and 24 in the hSlo$\Delta_{579-664}$ variant. Inclusion of exons 18, 19, or 23 alone (constructs e18, e19, or e23) did not rescue any cell surface expression of the hSlo$\Delta_{579-664}$ variant. Similarly, inclusion of exon 19 with exon 23 (e19 + e23) or exon 18 with exon 23 (e18 + e23) did not rescue cell surface expression of the hSlo$\Delta_{579-664}$ variant. In contrast, inclusion of both exons 18 and 19 (e18 + e19) partially rescued cell surface expression in both quantitative immunofluorescence assays (Fig. 4*a*) as well cell surface biotinylation assays (Fig. 4*b*). These data suggest that: (i) exon 23 is not essential *per se* for cell surface expression; (ii) the length of the amino acid insertion *per se* is not important for cell surface expression; and (iii) exons 18 and 19 are required for cell surface expression, and thus their exclusion is likely to result in loss of putative trafficking signals.

An Acidic Cluster Motif in the RCK1-RCK2 Linker Is Required for Cell Surface Expression—To further refine our analysis, we aligned exons 18 and 19 from the zero variants of BK channel orthologs from man to flies (Fig. 5*a*). This revealed the high conservation of this region that spans the very C terminus of the computationally predicted RCK1 domain and the start of the unstructured (NORS) RCK1-RCK2 linker region (18).

Examination of the amino acid sequence encoded by exons 18, 19, and 23 (Fig. 5*a*) revealed three regions that may act as putative trafficking motifs: (i) The junction of exon 16 and exon 18 encodes a putative TGN-endosome trafficking signal in vertebrate BK channels (E*XXX*LI) similar to the consensus (D/E)*XXX*L(L/I). However, (D/E)*XXX*L(L/I) motifs show considerable degeneracy (28) with an R*XXX*LL signal exploited in the Glut4 transporter (29) and an E*XXX*LI motif in AQP4 (30). (ii) Exon 19 encodes a putative acidic cluster signal DD*XX*D that is important for trafficking of a number of potassium channels (22, 31–34). In addition, the acidic cluster may also form part of a D*XX*LL-like motif (D*XXX*I) that is predicted (using the PredictProtein server; data not shown) to form a short α-helical structure. Intriguingly, such a short α-helical region is commonly observed in other ER exit signals with little primary sequence homology (16, 35) and is predicted to play an important role in the more C-terminal ER exit signal in BK channels (16). Furthermore, this short α-helical region represents the only computationally predicted structured region in the otherwise unstructured NORS (no regular secondary structure) RCK1-RCK2 linker (18) conserved from man to flies. (iii) The very 5′ start of exon 23 encodes another putative acidic motif (EDE) that is conserved in vertebrates.

We took a site-directed mutagenesis approach using the zero variant to examine the contribution of these putative trafficking signals in BK channel cell surface expression (Fig. 5, *b* and *c*). Mutation of Glu^{576} or of Leu^{580} and Ile^{581} to alanine to disrupt the E*XXX*LI motif at the exon 16-exon 18 junction, as well as alanine mutation of the EDE motif in exon 23, significantly reduced cell surface labeling of the zero variant in imaging assays but did not abolish it (Fig. 5*c*). Furthermore, a combination of mutations at both sites did not abolish cell surface labeling, because expression was still 20.1 ± 4.2% of the zero variant.

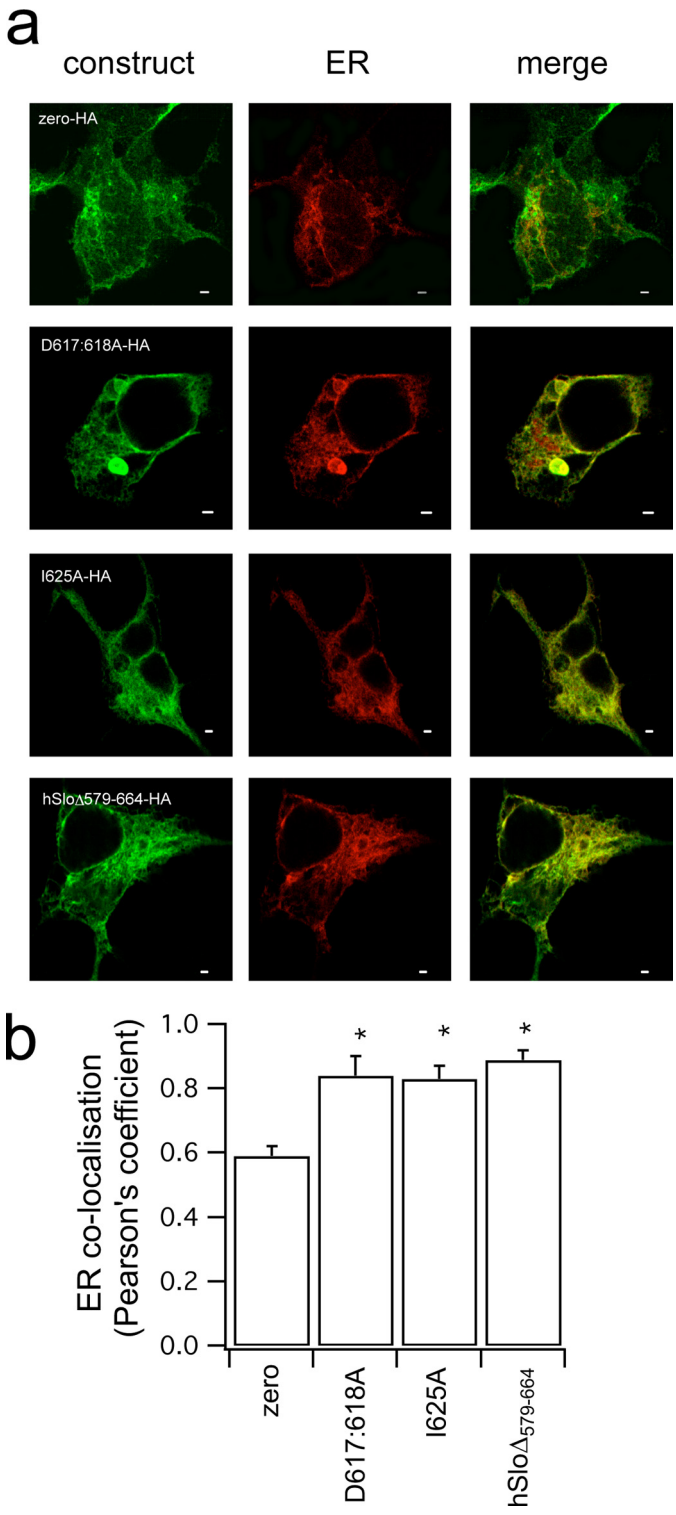

FIGURE 6. **Trafficking-deficient BK channel mutants are trapped in the ER.** *a*, representative single confocal sections from permeabilized cells co-transfected with the corresponding HA-tagged BK channel site-directed mutant (construct, *green*) and the endoplasmic reticulum marker expression plasmid pdsRed-ER (*ER*, *red*). The merged images are shown in the *right-hand panels*. *b*, summary bar graph of Pearson's correlation coefficient for quantitative co-localization of the respective HA-tagged channels with the pdsRed-ER marker (a value of 1.0 would indicate complete co-localization). *, $p < 0.05$, ANOVA with post hoc Dunnett's test compared with the zero channel.

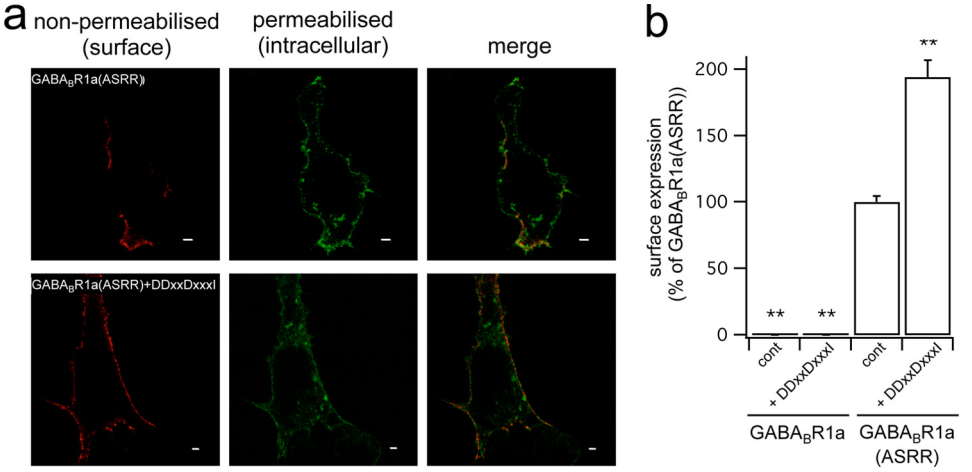

FIGURE 7. **Acidic cluster sequence (DD*XX*D*XXX*I) is a transplantable ER export motif.** *a*, representative single confocal sections from HEK293 cells expressing the GABA$_B$R1a receptor with (*GABA$_B$R1a(ASRR)+DDXXDXXXI*) and without (*GABA$_B$R1a(ASRR)*) the DD*XX*D*XXX*I motif engineered onto the C terminus. The N-terminal (extracellular) HA epitope tag was labeled under nonpermeabilized (*left panels*, *red*) and permeabilized (*middle panels*, *green*) conditions in the same cell with the merged images shown in the *right-hand panels*. The GABA$_B$R1a receptor contained an arginine to alanine mutation (ASRR) compared with the wild type GABA$_B$R1a receptor. The *scale bars* are 2 μm. *b*, summary bar graph of quantitative surface/intracellular HA expression normalized to the ratio for the GABA$_B$R1a(ASRR) expressing cells (100%). **, $p < 0.01$, ANOVA with post hoc Dunnett's test compared with the zero channel (n = 16–19/group).

In contrast, mutation of the DD*XX*D*XXX*I motif (D617A/D618A or I625A constructs) completely abolished cell surface labeling in imaging assays as with the hSlo$\Delta_{579-664}$ variant (Fig. 5, *b* and *c*). To confirm the lack of cell surface expression in these mutants, we also performed cell surface biotinylation assays (Fig. 5, *d* and *e*). Mutation of the DD*XX*D*XXX*I motif (D617A/D618A mutant) again abolished cell surface expression as for the hSlo$\Delta_{579-664}$ splice variant. In contrast, mutation of the E*XXX*LI or EDE motifs (E576A or E634A/D635A/E636A, respectively) significantly reduced but did not abolish cell surface expression of the channel (Fig. 5, *d* and *e*). However, because mutation of the EDE motif alone significantly reduced surface expression, this would suggest that the inability to fully rescue surface expression with the e18 + e19 construct in Fig. 4 is a result of the loss of the EDE sequence within exon 23 in the e18 + e19 construct. Mutation of the DD*XX*D*XXX*I motif also completely abolished cell surface labeling in the e18 + e19 construct, further confirming the essential requirement for this sequence (not shown).

The mutant channels were now predominantly ER-localized as determined by co-localization assays (Fig. 6, *a* and *b*). We determined the Pearson's correlation coefficient in quantitative immunofluorescence imaging assays with the channel constructs upon co-expression with the ER marker pdsRed-ER (Clontech). For the zero variant the coefficient was 0.59 ± 0.05, which was significantly (ANOVA, post hoc Dunnett's test $p <$ 0.01) increased with the hSlo$\Delta_{579-664}$ variant as well as the D617A/D618A and I625A mutants (Fig. 6*b*), demonstrating trapping of these mutants in the ER.

Because the DD*XX*D*XXX*I acidic-like motif plays a dominant role in determining cell surface expression, we thus asked whether this motif could function as a transplantable trafficking signal. We exploited the GABA$_B$R1a receptor (a nonchannel subunit of the G-protein-coupled receptor for the γ-aminobutyric acid neurotransmitter), which is normally retained in the ER by a R*XX*RR-dependent ER retrieval and retention mechanism to examine whether the DD*XX*D*XXX*I motif could enhance cell surface expression of the receptor as for acidic trafficking motifs identified in other potassium channels (22). We engineered the DD*XX*D*XXX*I motif onto the intracellular C terminus of the GABA$_B$R1a receptor and monitored cell surface to intracellular expression by probing for the extracellular N-terminal HA tag under nonpermeablized and permeabilized conditions using quantitative immunofluorescence (Fig. 7). In agreement with previous studies (22), the DD*XX*D*XXX*I motif could not rescue surface expression of the wild type GABA$_B$R1a receptor (Fig. 7*b*). However, in GABA$_B$R1a receptors with an arginine to alanine point mutation in its ER retention/retrieval R*XX*RR motif (ASRR mutant), surface expression of the GABA$_B$R1a receptor was now detectable. Importantly, surface expression was significantly enhanced (almost 2-fold) by transplanting the DD*XX*D*XXX*I motif from the BK channel. Thus the DD*XX*D*XXX*I sequence cannot override the ER retention/retrieval signal but can accelerate ER export in the absence of the R*XX*RR motif as demonstrated for other acidic ER export signals from inwardly rectifying potassium channels (22). To verify that the D617A/D618A and I625A mutations resulted in a significant reduction of functional BK channel expression at the plasma membrane, we exploited a membrane potential assay (24) to interrogate BK channel activation in response to ionomycin-induced (1 μM) calcium influx in HEK293 cells using the voltage-sensitive dye FLIPR blue (Molecular Devices). In response to ionomycin HEK293 cells, expressing the functional zero channel variant elicited a robust hyperpolarization compared with mock transfected HEK293 cells (Fig. 8*a*). No significant hyperpolarization in membrane potential was observed in cells expressing hSlo$\Delta_{579-664}$ (Fig. 8). Membrane hyperpolarization was significantly attenuated (to less than 40% of zero) in cells expressing either the D617A/D618A or the I625A mutant in line with the reduced membrane expression in imaging assays. The residual hyperpolarization with both mutants suggests that low numbers of D617A/D618A and I625A channels may reach the cell surface and that this level is below the limit of detection in our cell surface labeling assays. Taken together, these data reveal that the acidic cluster-like motif in exon 19 represents a transplantable trafficking motif that plays a critical role in controlling cell surface expression of BK channels.

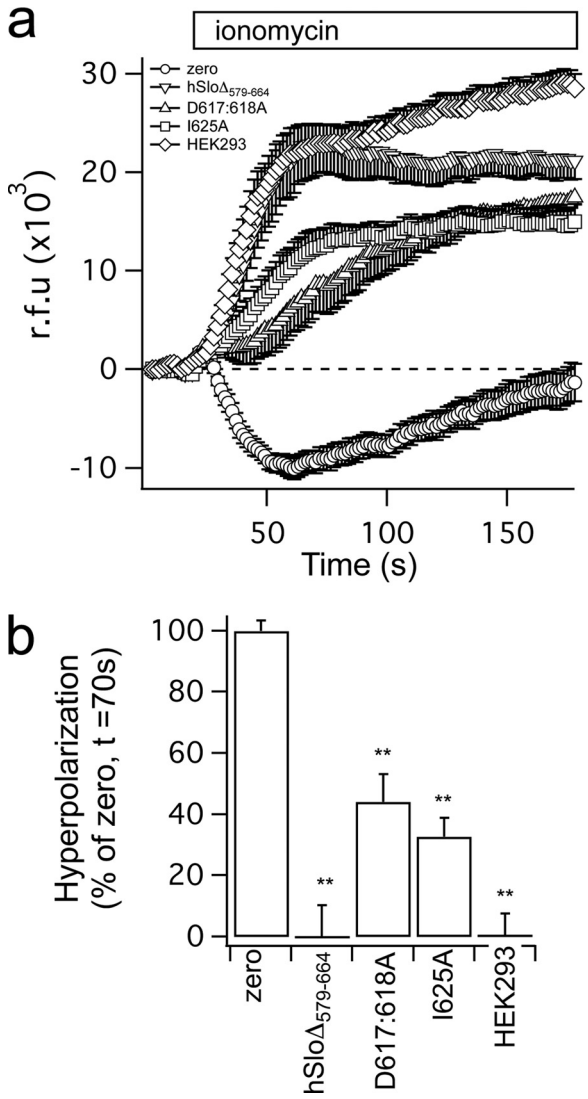

FIGURE 8. **Acidic cluster sequence (DD*XX*D*XXX*I) is required for efficient functional channel expression.** *a*, time course plots of change in relative fluorescence units (*r.f.u*) of the FLIPR blue membrane potential dye in HEK293 cells expressing zero (○), hSlo$\Delta_{579-664}$ (▽), D617A/D618A (△), I625A (■), or mock transfected HEK293 cells (◇) in response to calcium influx induced by 1 μM ionomycin. A decrease in fluorescence relative to the HEK293 cell response indicates a net hyperpolarization of the membrane potential resulting from activation of BK channels. *b*, summary bar chart of the membrane potential change for each construct in *a* expressed as a percentage of the maximal hyperpolarization elicited in HEK293 cells expressing the zero variant (100%). The data were determined at $t = 70$ s in the time course plots in *a*. All of the data are the means ± S.E. (n = 9–12). **, $p < 0.01$, ANOVA with post hoc Dunnett's test compared with the zero channel response.

DISCUSSION

We have identified three distinct motifs within the intracellular RCK1-RCK2 linker of BK channels that control their cell surface expression. In particular, an acidic cluster-like motif, DD*XX*D*XXX*I, is critical for cell surface expression and is highly conserved from flies to man. This acidic motif can be transplanted to nonchannel proteins to accelerate ER export but cannot override pre-existing ER retention signals, as described for other acidic motifs (22). Importantly, alternative splicing of a human BK channel splice variant hSlo$\Delta_{579-664}$ that excludes the exons encoding this motif results in a trafficking-deficient BK channel that acts as a dominant negative for cell surface expression.

The DD*XX*D*XXX*I motif may comprise both an acidic cluster motif as well as a degenerate D*XX*LL motif. Indeed in worms and flies, a D*XX*LI motif is retained, whereas the third position is an arginine in vertebrates. Thus, although the motif does not share sequence conservation with other trafficking motifs, it is intriguing that the D*XXX*I motif is predicted to form a short α-helix at the very beginning of the predicted linker region that otherwise lacks a regular secondary structure (18). A short α-helical structure is a feature commonly associated with ER export signals that do not show sequence homology (16, 35) as suggested for the more C-terminal ER export sequence in BK channels (16). Acidic cluster motifs are also commonly used as ER export signals, including in other potassium channels (22, 31, 33, 34). These features also appear crucial for cell surface expression of BK channels. In contrast, the EDE acidic cluster in exon 23 is not essential for surface expression, but mutagenesis does significantly reduce it. Similar acidic clusters have been reported in other transmembrane proteins including inwardly rectifying and TASK3 potassium channels (22, 31, 33, 34). The E*XXX*LI motif is most likely a member of the (D/E)*XXX*L(L/I) sorting motif that shows considerable degeneracy; in fact, in AQP4 channels an E*XXX*LI motif is essential for correct trafficking (30).

The demonstration here of *exclusion* of the ER export DD*XX*D*XXX*I acidic motif by alternative splicing in the intracellular C-terminal linker of BK channels nicely contrasts with the *inclusion* of an hydrophobic (CVLF) ER retention signal through alternative splicing of the N-terminal intracellular S0-S1 loop of BK channels (12). Taken together, these data strongly support the hypothesis that alternative splicing plays a major role in controlling cell surface expression of ion channels and that this can be achieved in the same channel by diametrically opposite mechanisms: through either exclusion or inclusion of cognate trafficking motifs.

Why do BK channels have multiple trafficking motifs whose inclusion can be controlled by alternative splicing? Because BK channels have pleitropic functions in virtually all tissues of the body, it is likely that multiple trafficking and sorting signals are required to allow the correct surface expression and subcellular localization of BK channels relevant to the target tissue of interest. Furthermore, increasing evidence suggests that cell surface expression of BK channels is dynamically regulated, both through signals that may regulate splicing and through post-translational modifications and assembly with distinct regulatory β-subunits. Thus these multiple mechanisms are likely coordinated to expose or mask the correct complement of trafficking and sorting signals to allow appropriate distribution of BK channels within distinct cell types. Indeed, alternative splicing of the rat SVcyt ortholog of hSlo$\Delta_{579-664}$ is dynamically regulated in corporeal tissue in models of diabetes (17). Whether the dominant negative function of hSlo$\Delta_{579-664}$ is physiologically relevant in this or other model systems remains to be explored. Clearly the inclusion (13, 27) or exclusion (as observed with the hSlo$\Delta_{579-664}$ variant here) of trafficking motifs through alternative splicing most likely represents a fundamental mechanism for controlling BK channel cell sur-

face expression under a variety of physiological and pathophysiological conditions.

Acknowledgments—We thank Heather McClafferty and Lijun Tian and other members of the respective laboratories for critical discussions during this work and Trudi Gillespie and the IMPACT imaging facility for assistance in confocal imaging assays. The $GABA_{BR}1a$ receptor wild type and ASRR constructs were generous gifts from Lily Jan (University of California at San Francisco).

REFERENCES

1. Sausbier, M., Arntz, C., Bucurenciu, I., Zhao, H., Zhou, X. B., Sausbier, U., Feil, S., Kamm, S., Essin, K., Sailer, C. A., Abdullah, U., Krippeit-Drews, P., Feil, R., Hofmann, F., Knaus, H. G., Kenyon, C., Shipston, M. J., Storm, J. F., Neuhuber, W., Korth, M., Schubert, R., Gollasch, M., and Ruth, P. (2005) *Circulation* **112,** 60–68
2. Brenner, R., Peréz, G. J., Bonev, A. D., Eckman, D. M., Kosek, J. C., Wiler, S. W., Patterson, A. J., Nelson, M. T., and Aldrich, R. W. (2000) *Nature* **407,** 870–876
3. Raffaelli, G., Saviane, C., Mohajerani, M. H., Pedarzani, P., and Cherubini, E. (2004) *J. Physiol.* **557,** 147–157
4. Sausbier, M., Hu, H., Arntz, C., Feil, S., Kamm, S., Adelsberger, H., Sausbier, U., Sailer, C. A., Feil, R., Hofmann, F., Korth, M., Shipston, M. J., Knaus, H. G., Wolfer, D. P., Pedroarena, C. M., Storm, J. F., and Ruth, P. (2004) *Proc. Natl. Acad. Sci. U.S.A.* **101,** 9474–9478
5. Du, W., Bautista, J. F., Yang, H., Diez-Sampedro, A., You, S. A., Wang, L., Kotagal, P., Lüders, H. O., Shi, J., Cui, J., Richerson, G. B., and Wang, Q. K. (2005) *Nat. Genet.* **37,** 733–738
6. Meredith, A. L., Thorneloe, K. S., Werner, M. E., Nelson, M. T., and Aldrich, R. W. (2004) *J. Biol. Chem.* **279,** 36746–36752
7. Werner, M. E., Zvara, P., Meredith, A. L., Aldrich, R. W., and Nelson, M. T. (2005) *J. Physiol.* **567,** 545–556
8. Song, M., Zhu, N., Olcese, R., Barila, B., Toro, L., and Stefani, E. (1999) *FEBS Lett.* **460,** 427–432
9. Marijic, J., Li, Q., Song, M., Nishimaru, K., Stefani, E., and Toro, L. (2001) *Circ. Res.* **88,** 210–216
10. Sørensen, M. V., Matos, J. E., Sausbier, M., Sausbier, U., Ruth, P., Praetorius, H. A., and Leipziger, J. (2008) *J. Physiol.* **586,** 4251–4264
11. Butler, A., Tsunoda, S., McCobb, D. P., Wei, A., and Salkoff, L. (1993) *Science* **261,** 221–224
12. Zarei, M. M., Eghbali, M., Alioua, A., Song, M., Knaus, H. G., Stefani, E., and Toro, L. (2004) *Proc. Natl. Acad. Sci. U.S.A.* **101,** 10072–10077
13. Korovkina, V. P., Brainard, A. M., and England, S. K. (2006) *J. Physiol.* **573,** 329–341
14. Ma, D., Nakata, T., Zhang, G., Hoshi, T., Li, M., and Shikano, S. (2007) *FEBS Lett.* **581,** 1000–1008
15. Chen, L., Tian, L., MacDonald, S. H., McClafferty, H., Hammond, M. S., Huibant, J. M., Ruth, P., Knaus, H. G., and Shipston, M. J. (2005) *J. Biol. Chem.* **280,** 33599–33609
16. Kwon, S. H., and Guggino, W. B. (2004) *Proc. Natl. Acad. Sci. U.S.A.* **101,** 15237–15242
17. Davies, K. P., Zhao, W., Tar, M., Figueroa, J. C., Desai, P., Verselis, V. K., Kronengold, J., Wang, H. Z., Melman, A., and Christ, G. J. (2007) *Eur. Urol.* **52,** 1229–1237
18. Lee, J. H., Kim, H. J., Kim, H. D., Lee, B. C., Chun, J. S., and Park, C. S. (2009) *Biophys. J.* **97,** 730–737
19. Tian, L., Jeffries, O., McClafferty, H., Molyvdas, A., Rowe, I. C., Saleem, F., Chen, L., Greaves, J., Chamberlain, L. H., Knaus, H. G., Ruth, P., and Shipston, M. J. (2008) *Proc. Natl. Acad. Sci. U.S.A.* **105,** 21006–21011
20. Tian, L., Coghill, L. S., McClafferty, H., MacDonald, S. H., Antoni, F. A., Ruth, P., Knaus, H. G., and Shipston, M. J. (2004) *Proc. Natl. Acad. Sci. U.S.A.* **101,** 11897–11902
21. Tian, L., Duncan, R. R., Hammond, M. S., Coghill, L. S., Wen, H., Rusinova, R., Clark, A. G., Levitan, I. B., and Shipston, M. J. (2001) *J. Biol. Chem.* **276,** 7717–7720
22. Ma, D., Zerangue, N., Lin, Y. F., Collins, A., Yu, M., Jan, Y. N., and Jan, L. Y. (2001) *Science* **291,** 316–319
23. Rickman, C., Medine, C. N., Bergmann, A., and Duncan, R. R. (2007) *J. Biol. Chem.* **282,** 12097–12103
24. Saleem, F., Rowe, I. C., and Shipston, M. J. (2009) *Br. J. Pharmacol.* **156,** 143–152
25. Yusifov, T., Savalli, N., Gandhi, C. S., Ottolia, M., and Olcese, R. (2008) *Proc. Natl. Acad. Sci. U.S.A.* **105,** 376–381
26. Xu, W., Liu, Y., Wang, S., McDonald, T., Van Eyk, J. E., Sidor, A., and O'Rourke, B. (2002) *Science* **298,** 1029–1033
27. Zarei, M. M., Zhu, N., Alioua, A., Eghbali, M., Stefani, E., and Toro, L. (2001) *J. Biol. Chem.* **276,** 16232–16239
28. Bonifacino, J. S., and Traub, L. M. (2003) *Annu. Rev. Biochem.* **72,** 395–447
29. Sandoval, I. V., Martinez-Arca, S., Valdueza, J., Palacios, S., and Holman, G. D. (2000) *J. Biol. Chem.* **275,** 39874–39885
30. Madrid, R., Le Maout, S., Barrault, M. B., Janvier, K., Benichou, S., and Mérot, J. (2001) *EMBO J.* **20,** 7008–7021
31. Ma, D., Zerangue, N., Raab-Graham, K., Fried, S. R., Jan, Y. N., and Jan, L. Y. (2002) *Neuron* **33,** 715–729
32. Mikosch, M., Käberich, K., and Homann, U. (2009) *Traffic* **10,** 1481–1487
33. Taneja, T. K., Mankouri, J., Karnik, R., Kannan, S., Smith, A. J., Munsey, T., Christesen, H. B., Beech, D. J., and Sivaprasadarao, A. (2009) *Hum. Mol. Gen.* **18,** 2400–2413
34. Zuzarte, M., Rinné, S., Schlichthörl, G., Schubert, A., Daut, J., and Preisig-Müller, R. (2007) *Traffic* **8,** 1093–1100
35. Sevier, C. S., Weisz, O. A., Davis, M., and Machamer, C. E. (2000) *Mol. Biol. Cell* **11,** 13–22